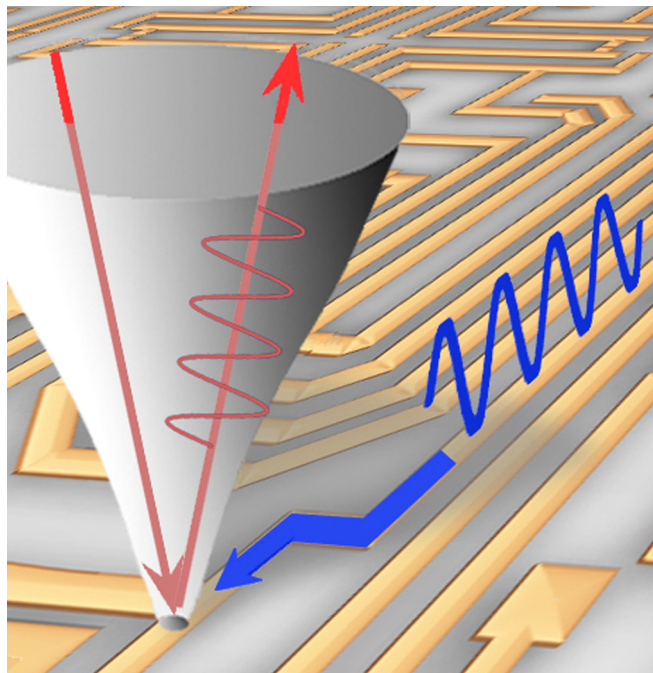


Tapered and Tip-Grounded Waveguide Electrooptical Microsensors

Volume 3, Number 1, February 2011

Ru-Long Jin
Han Yang
Di Zhao
Feng Zhu
Yan-Hao Yu
Qi-Dai Chen
Mao-Bin Yi
Hong-Bo Sun, Member, IEEE



DOI: 10.1109/JPHOT.2010.2101588
1943-0655/\$26.00 ©2011 IEEE

Tapered and Tip-Grounded Waveguide Electrooptical Microsensors

Ru-Long Jin,¹ Han Yang,¹ Di Zhao,¹ Feng Zhu,¹ Yan-Hao Yu,¹ Qi-Dai Chen,¹
Mao-Bin Yi,¹ and Hong-Bo Sun,^{1,2} *Member, IEEE*

¹State Key Laboratory on Integrated Optoelectronics, College of Electronic Science and Engineering,
Jilin University, Changchun 130023, China

²College of Physics, Jilin University, Changchun 130012, China

DOI: 10.1109/JPHOT.2010.2101588
1943-0655/\$26.00 ©2011 IEEE

Manuscript received November 23, 2010; revised December 12, 2010; accepted December 13, 2010.
Date of publication December 18, 2010; date of current version January 24, 2011. This work was
supported by the National Scientific Foundation of China under Grant 61077002 and Grant 90923037
and by the 863 program under Grant 2009AA03Z401. Corresponding authors: H. B. Sun (e-mail:
hbsun@jlu.edu.cn) and H. Yang (yanghan@jlu.edu.cn).

Abstract: A tip-grounded waveguide microsensor was proposed to overcome the difficulty of quantitative voltage calibration in electrooptical detection for integrated circuit (IC) test. On this basis, we optimized the thickness of the electrooptical material of the sensor to eliminate the influence of the circuit layout on the measured signals. The improved sensor in return made it possible to calibrate the voltage with known reference electric signals quantitatively. This method circumvented the uncertainty of the probe conditions of each measurement point. Finally, a calibration accuracy of better than 6% was obtained, which satisfied broad applications in the IC industry.

Index Terms: Electrooptic modulation, electric field measurement, electrooptic effects, voltage calibration, semiconductor device testing.

1. Introduction

Electrooptical detection is now being considered as a powerful and attractive option for high-precision local electric field measurement, primarily due to its unique merits like large intrinsic bandwidths (DC to THz), noninvasiveness, and high response speed [1], [2]. The core component of an electrooptical probe is a tiny piece of electrooptical film consisting either of polymers [3]–[5] or semiconductor crystals [6]–[9], affixed to the tip of a tapered waveguide. If the optical performance of the film, e.g., refractive index or birefringence, is affected by external electric field, the probe is feasibly implemented as a proximity electric field sensor, functioning when it is brought to the immediate surface of an integrated circuit (IC). The waveform of the electric signal at a particular site of the IC is thus attainable by measuring the phase modulation of a laser beam traveling through the film on the probe. This makes the electrooptical detection a promising tool for IC fault diagnosis and design improvement [10], [11]. Nevertheless, a drawback of the method that is hindering its practical use is the inherent difficulty in calibrating the voltage magnitude [12]. Although some proposals try to overcome the complexity [13]–[15], they are not applicable to the electrooptical detection using an external probe. It is difficult to correctly determine the value of the applied voltage because of the emanating field divergence from an IC circuit line and the uncertainty of the physical contact between the probe tip and the circuit. The former, which is associated with the IC layout, local routing, line width, and spacing, is caused by interruption of neighbored nodes or lines. The latter is inevitable in different runs of each voltage measurement

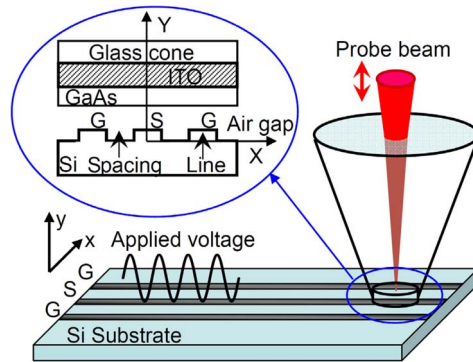


Fig. 1. Electrooptical probing. The inset is the cross section of the schematic probe tip with a conductive film inserted, where G and S separately represent the ground and signal line of the coplanar waveguide circuit.

process [8] since no appropriate and fine distance monitoring or feedback mechanism has been found for such a system. In this letter, we solved the problem by introducing a transparent conductive film between the tapered waveguide and the electrooptical film. First, if the conductive film is grounded and the electrooptical film is thin enough, the fringing electric field of the circuit line would not be attracted by the neighbored nodes or lines but by the microelectrode. Second, loading with known reference electric signals, the microelectrode enables precise measurement of voltages in the close vicinity of the IC surface.

2. Principle and Simulations

Fig. 1 illustrates tapered and tip-ground waveguide electrooptical microsensors. For optical probing of ICs, the sensor is brought directly to the region of the fringing field from the transmission lines along which electric signals propagate [16], [17]. The output optical signals are determined by the phase modulation depth $\Delta\phi$, which is associated with the voltage fall across the electrooptical film V by $\Delta\phi = (2\pi/\lambda)n_0^3\gamma_{ij}V$ [7], [12], where γ_{ij} is the electrooptical tensors, n_0 is the refractive index, and λ is the probing beam wavelength. In practice, the voltage fall is not quantitatively related with the local voltage V_{IC} . This can be understood with a potential simulation in the proximity of the circuit surface, which can be obtained by calculating the following differential equation:

$$\nabla(\varepsilon\nabla\Phi) = 0 \quad (1)$$

where Φ is the potential, and ε is the dielectric constant. The simultaneous equations of different boundary conditions (electrooptical film, circuit substrate, and air gap) were solved numerically by the finite element method [12], [18]. Moreover, by analyzing the field distribution, the function of the conductive film mentioned above can be recognized clearly.

For this simulation, a coplanar waveguide circuit of line width $\delta_{line} = 1 \mu\text{m}$ and a GaAs electrooptical film of thickness $\delta_{eofilm} = 10 \mu\text{m}$ was adopted. The air gap was assumed to be $\delta_{airgap} = 0.2 \mu\text{m}$ (see the inset of Fig. 1), which always exist because of circuit surface topography and the passivation layer [19] that prevents the probe tip from approaching it. The circuit voltage (V_{IC}) was assumed to be 1 V. The voltage falls across every point of the electrooptical film (V_{eofilm}) were simulated at line spacing of $\delta_{spacing} = 0.2, 0.5, 1.0, 2.0,$ and $5.0 \mu\text{m}$, respectively. As seen from Fig. 2(a), the voltage difference distribution along x-axis (see the inset of Fig. 1) depends sensitively on $\delta_{spacing}$. For the purpose of eliminating interference from neighboring lines, a conductive film was introduced and grounded to aid directional alignment of the entire fringing field from the transmission lines to it. Since the range of fringing field is generally limited to within several micrometers, in order to bring the microelectrode into play, δ_{eofilm} needs optimizing. As shown in

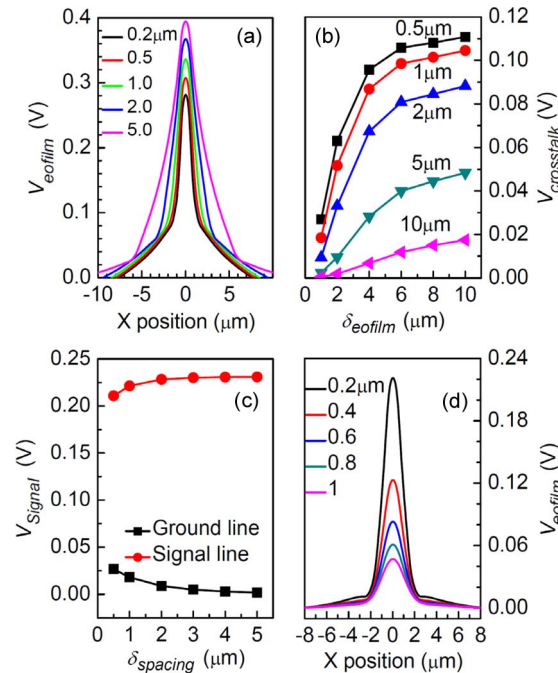


Fig. 2. Simulation of the voltage falls across the electrooptical film of the probe by finite element technique. (a) The voltage difference distribution along the x -axis position depends on the spacing of the transmission lines ($\delta_{spacing}$), where x position is the location of the x -axis in the inset of Fig. 1. (b) The voltage falls above the ground line $V_{crosstalk}$ decreases versus the reduction of the crystal thickness at different line spacing ($\delta_{spacing}$). (c) The influence of $\delta_{spacing}$ on the voltage falls can be negligible by thinning the electrooptical film to $1 \mu\text{m}$, and the red and black lines present the voltage fall above the center of the signal and ground line separately. (d) The voltage difference distribution sensitively depends on the distance between the probe and the circuit.

Fig. 2(b), the voltage falling onto the electrooptical film above a grounded line, the crosstalk ($V_{crosstalk}$), which means the interruption of neighbored nodes or lines, which is expected to be ~ 0 , appeared as non-zero. The crosstalk decreases versus the reduction of δ_{eofilm} and enlargement of line spacing $\delta_{spacing}$. Thus, $\delta_{eofilm} \leq \delta_{spacing}$ was found a critical condition for realizing the function of the grounded electrode. For instance, for $\delta_{eofilm} \sim 1 \mu\text{m}$ for the mentioned circuit, the influence of circuit layout becomes negligible [see Fig. 2(c)], since the voltage fall above the center of the signal line (V_{signal}) becomes independent on line spacing, and $V_{crosstalk} \rightarrow 0$. As another obstacle for the voltage calibration, the effect of δ_{airgap} is confirmed [see Fig. 2(d)], proving that a tiny change of the gap gives rise to significant influence on the voltage distribution.

3. Experiments

The conductive film, which is chosen with further consideration of the requirement of the intensity of electrooptical signal strength, was achieved by sputtering an indium tin oxide (ITO) film [20] on a synthetic fused silica cone as waveguide [see the inset of Fig. 3(a)]. On the side face of the tapered waveguide, a 100-nm Au film utilized for electric connection of the ITO film to ground was first evaporated. As a transparent conductive microelectrode, the transmittance, conductivity, and flatness of the ITO film are the most important properties to study. Well-controlled sputtering parameter results finally in negligible transmission loss at the probe beam wavelength (1310 nm), which is less than 3%, including the intrinsic absorption [see Fig. 3(a)], when the film was about 320 nm thick. At this thickness, the sheet resistance of the conductive film is around $70 \Omega/\square$ [see Fig. 3(b)], which is far below that of GaAs film as the electrooptical film and, therefore, is negligible. Thus, the electrooptical film was reasonably considered to be directly grounded. The average roughness of the film, measured by an atomic force microscope, was about 3 nm [see the inset of

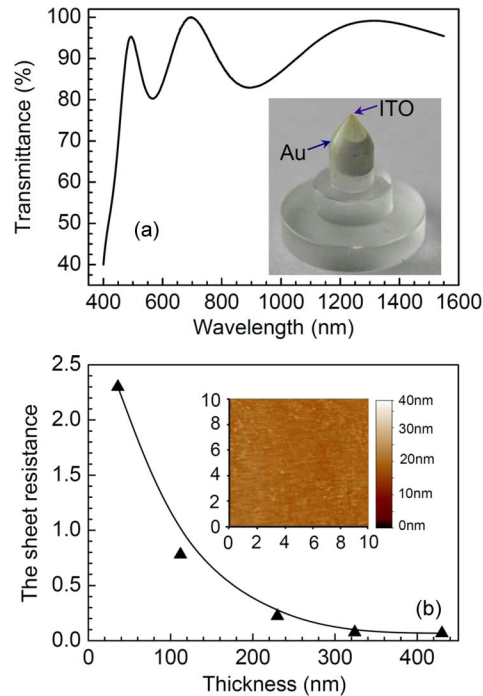


Fig. 3. Characteristics of the ITO film functioning as a transparent conductive electrode. (a) The transmittance and (b) sheet resistance ($K\Omega/\square$) of the electrode. The insets separately show the probe and its surface topography measured by atom force microscope.

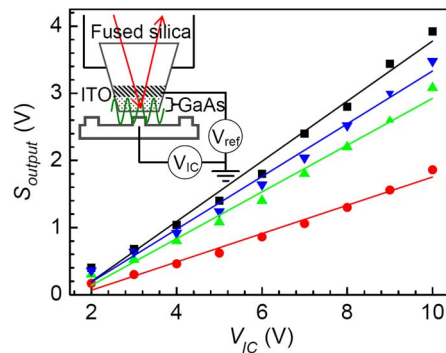


Fig. 4. Linear dependence of the output modulation signal on the local voltage of the circuit. The inset shows the specific implementation schematic of the new voltage calibration method.

Fig. 3(b)]. As a consequence, the influence of topography on voltage detection could be neglected. Finally, a double side optically polished $1\text{-}\mu\text{m}$ thick $\langle 100 \rangle$ -cut semi-insulating GaAs single crystal was affixed on the silica cone for field sensing, constituting an electrooptical sensor.

4. Result and Discussions

The improved electrooptic probe was then installed on a fine micropositioner to locate the measurement points to be detected. A 10-kHz sinusoid voltage was applied to the coplanar waveguide. The signals picked by the electrooptical sensor (S_{output}) were found linearly dependent on the input if the position of the sensor was spatially fixed (see Fig. 4). However, the slopes of the lines varied with different runs of tip-circuit approaching operations or with altered positions along a

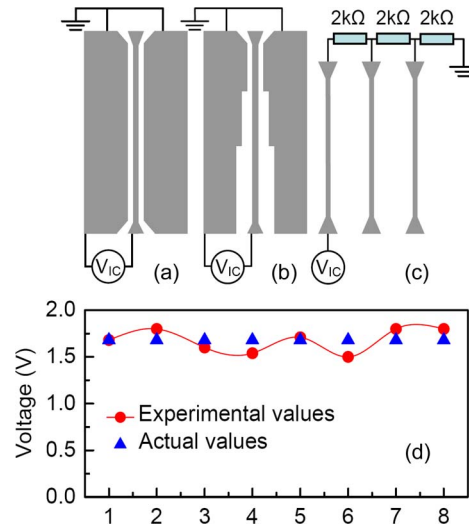


Fig. 5. Voltage calibration confirmatory experiments. (a)–(c) Three coplanar waveguide circuits were designed for certifying the calibration idea. (d) The measurement results of the circuit in part (a). The actual values were measured by the oscilloscope directly, while the experimental values were measured by electrooptical detection with voltage calibration procedure.

transmission line. This manifests the 3-D feature of the voltage distribution above the close vicinity of an IC surface, making the voltage calibration complicated.

The matter can actually be simplified if calibration is performed not on various voltages of an operating circuit but on the microsensor itself. By careful examinations of Fig. 4, one finds S_{output} is associated with the voltage applied to the circuit V_{IC} by a constant κ through

$$S_{output} = \kappa(V_{IC} - \nu) \quad (2)$$

where κ reflects the system sensitivity, and ν is the minimum voltage loading on the circuit which could be detected by the system. The relation stands true (κ and ν are fixed) as long as the probe location relative to the circuit is invariable. This implies that if the voltages loaded on the electrooptical film are known, it would be easy to determine the probe system constants at that measurement point κ and ν by solving simultaneous equations. Therefore, we introduce the reference signals to the ITO film. The output signal we measured is induced by the superimposed signal of the circuit and reference electric signals. Besides, because the reference signals are known and the linear relation between the output signal and the voltage falls across the electrooptical film, it is convenient to figure out the circuit voltage value. This process can be carried out by software for each point as a necessary measurement procedure. This, in return, makes it possible to calibrate the voltage point by point at IC surface.

Three coplanar waveguides [see Fig. 5(a)] were designed to certify whether the idea above was feasible. The frequency and phase of the circuit electric signal were detected with the tip-grounded sensor beforehand, which could determine the frequency and phase of the reference signals. When the sensor was then utilized to measure the electric signal of the coplanar waveguide, the circuit electric signal was monitored by the oscilloscope directly as a comparison. Eight points were randomly chosen on the signal line of the circuit [see Fig. 5(a)], and the standard deviation was found to be less than 6% [see Fig. 5(d)] by this calibration procedure. The average of the eight experiment values is 1.67 V [see Fig. 5(d)], which is close to the actual value 1.68 V; therefore, we can get higher accuracy by averaging the values of several measurements. Such accuracy satisfies the demands of IC detection for fault diagnosis, such as troubleshooting functional and physical defects. Especially, the physical defects, i.e., bridging shorts, gate oxide defects, and open defects [21], generally give rise to significant changes of electric signals. The circuit in Fig. 5(b) was used to

TABLE 1
Measurement values of the circuits to be detected

	V_{IC} (V)	V_1 (V)	V_2 (V)	V_3 (V)
①	1.68	1.61	1.64	1.70
②	1.68	1.66	1.12	0.59

imitate a circuit with different spacing among transmission lines. As predicted in Fig. 2(a), different spacing between the measured line and its neighbored lines will smear the electric field distribution. In order to certify that the influence of the circuit layout has been eliminated in the proposed calibration method, we carried out measurements on the circuit Fig. 5(b). The same accuracy as the former case was obtained once more [see Table 1-①]. The third test was performed on a voltage divider circuit [see Fig. 5(c)], from which both the expected accuracy and theoretical ratio of 3 : 2 : 1 were attained [see Table 1-②]. The repeatability is important for this voltage-calibration method. We conducted experiments in different measurements with probes of different fabrications. As a result, the measured voltages show no probe dependence.

The capacitive effect of the inserted conductive film should be taken into account when the circuits under test are operating at high frequency. A GaAs film of 1 μm thickness with an electrode on its top loads the circuit with a capacitance of roughly 12 fF, functioning when the width of the transmission line is 1 μm . Such a capacitance can be neglected at the frequency of less than 1 GHz. Therefore, the electrode can apply to the signal frequency of 1 GHz. Although the working frequency of ICs may be much higher than 1 GHz, low-frequency or static detection is important to circumvent the effect of high-frequency parasitic parameters, especially for physical defects of ICs.

5. Conclusion

In summary, voltage calibration for electrooptical detection of ICs by field convergence with a tip-grounded waveguide microsensors was reported, by which measurement accuracy better than 6% has been achieved. The technology, which is expected to be a promising noninvasive IC diagnosis method, may work on the basis of not only electrooptic effect but also other sensing mechanisms [17] like linear (Pockel, inverse piezoelectric [22]) and nonlinear (Kerr, electrostrictive [23]) effects.

References

- [1] A. Garzarella, S. B. Qadri, T. J. Wieting, and D. H. Wu, "The effects of photorefractive on electro-optic field sensors," *J. Appl. Phys.*, vol. 97, no. 11, p. 113 108, Jun. 2005.
- [2] Q. Wu and X. C. Zhang, "Ultrafast electro-optic field sensors," *Appl. Phys. Lett.*, vol. 68, no. 12, pp. 1604–1606, Mar. 1996.
- [3] H. Cao, T. F. Heinz, and A. Nahata, "Electro-optic detection of femtosecond electromagnetic pulses by use of poled polymers," *Opt. Lett.*, vol. 27, no. 9, pp. 755–777, May 2002.
- [4] H. H. Fang, Q. D. Chen, J. Yang, H. Xia, Y. G. Ma, H. Y. Wang, and H. B. Sun, "Two-photon excited highly polarized and directional upconversion emission from slab organic crystals," *Opt. Lett.*, vol. 35, no. 3, pp. 441–444, Jan. 2010.
- [5] Q. D. Chen, H. H. Fang, B. Xu, J. Yang, H. Xia, F. P. Chen, W. J. Tian, and H. B. Sun, "Two-photon induced amplified spontaneous emission from needlelike triphenylamine-containing derivative crystals with low threshold," *Appl. Phys. Lett.*, vol. 94, no. 20, p. 201 113, May 2009.
- [6] O. Mitrofanov, A. Gasparyan, L. N. Pfeiffer, and K. W. West, "Electro-optic effect in an unbalanced AlGaAs/GaAs microresonator," *Appl. Phys. Lett.*, vol. 86, no. 20, p. 202 103, May 2005.
- [7] T. Nagatsuma, T. Shibata, E. Sano, and A. Iwata, "Subpicosecond sampling using a noncontact electro-optic probe," *J. Appl. Phys.*, vol. 66, no. 9, pp. 4001–4009, Nov. 1989.
- [8] O. Hollricher, F. Rudders, and C. Buchal, "Generation of guided polaritons in electro-optic LiTaO₃ probes," *J. Appl. Phys.*, vol. 77, no. 3, pp. 1903–1906, Feb. 1995.
- [9] X. Zheng, S. Wu, R. Sobolewski, R. Adam, M. Mikulics, P. Kordos, and M. Siegel, "Electro-optic sampling system with a single-crystal 4-N,N-dimethylamino-4'-N'-methyl-4-stilbazolium tosylate sensor," *Appl. Phys. Lett.*, vol. 82, no. 15, pp. 2383–2385, Apr. 2003.

- [10] M. Shinagawa and T. Nagatsuma, "A laser-diode-based picosecond electrooptic probe for high-speed LSI's," *IEEE Trans. Instrum. Meas.*, vol. 41, no. 3, pp. 375–380, Jun. 1992.
- [11] M. Shinagawa and T. Nagatsuma, "An automated electro-optic probing system for ultra-high-speed IC's," *IEEE Trans. Instrum. Meas.*, vol. 43, no. 6, pp. 843–847, Dec. 1994.
- [12] K. de Kort, A. Heringa, and J. J. Vreken, "The dependence of the electro-optic effect on electric field distribution and light beam propagation direction," *J. Appl. Phys.*, vol. 76, no. 3, pp. 1794–1799, Aug. 1994.
- [13] P. O. Muller, D. Erasme, and B. Huyart, "New calibration method in electrooptic probing due to wavelength control and Fabry–Perot resonance," *IEEE Trans. Microw. Theory Tech.*, vol. 47, no. 3, pp. 308–314, Mar. 1999.
- [14] D. R. Hjelme, M. J. Yadlowsky, and A. R. Mickelson, "Two-dimensional mapping of the microwave potential on MMIC's using electrooptic sampling," *IEEE Trans. Microw. Theory Tech.*, vol. 41, no. 6/7, pp. 1149–1158, Jun. 1993.
- [15] L. DuVillaret, J. M. Lourtioz, and L. Chusseau, "Absolute voltage measurements on III–V integrated circuits by internal electro-optic sampling," *Electron. Lett.*, vol. 31, no. 1, pp. 23–24, Jan. 1995.
- [16] H. F. Liu, M. B. Yi, H. B. Zhang, A. L. Hou, X. H. Chuai, and D. M. Zhang, "Electro-optic measurement system with high spatial resolution utilizing poled polymer film as external probe tip," *Opt. Laser Technol.*, vol. 37, no. 5, pp. 410–415, Jul. 2005.
- [17] R. L. Jin, H. Yang, D. Zhao, Q. D. Chen, Z. X. Yan, M. B. Yi, and H. B. Sun, "Optical probing of electric fields with an electro-acoustic effect towards integrated circuit diagnosis," *Opt. Lett.*, vol. 35, no. 4, pp. 580–582, Feb. 2010.
- [18] R. Hofmann and H. J. Pfeleiderer, "Simulations of the potential distribution and the resulting measurement signal in longitudinal external electro-optic probe tips," *Microelectron. Eng.*, vol. 31, no. 3, pp. 377–384, Feb. 1996.
- [19] T. W. O'Keeffe and M. W. Larkin, "Fabrication of semiconductor devices utilizing bombardment-enhanced etching of insulation layers," U.S. Patent 3 615 935, Oct. 26, 1971.
- [20] F. Kurdesau, G. Khripunov, A. F. da Cunha, M. Kaelin, and A. N. Tiwari, "Comparative study of ITO layers deposited by DC and RF magnetron sputtering at room temperature," *J. Non-Cryst. Solids*, vol. 352, no. 14, pp. 1446–1470, Jun. 2006.
- [21] R. Rajsuman, "Iddq testing for CMOS VLSI," *Proc. IEEE*, vol. 88, no. 4, pp. 544–566, Apr. 2000.
- [22] W. Shi, Y. J. Ding, X. Mu, X. Yin, and C. Fang, "Electro-optic and electromechanical properties of poled polymer thin film," *Appl. Phys. Lett.*, vol. 79, no. 23, pp. 3749–3751, Dec. 2001.
- [23] M. G. Kuzyk, J. E. Sohn, and C. W. Dirk, "Mechanisms of quadratic electro-optic modulation of dye-doped polymer systems," *J. Opt. Soc. Amer. B, Opt. Phys.*, vol. 7, no. 5, pp. 842–858, May 1990.